



OPEN

# Manipulating Complex Light with Metamaterials

SUBJECT AREAS:

METAMATERIALS  
OPTICAL PHYSICS

Jinwei Zeng, Xi Wang, Jingbo Sun, Apra Pandey, Alexander N. Cartwright &amp; Natalia M. Litchinitser

University at Buffalo, The State University of New York, Buffalo, New York 14260, USA.

Received  
6 August 2013Accepted  
13 September 2013Published  
2 October 2013Correspondence and  
requests for materials  
should be addressed to  
N.M.L. (natashal@  
buffalo.edu)

Recent developments in the field of metamaterials have revealed unparalleled opportunities for “engineering” space for light propagation; opening a new paradigm in spin- and quantum-related phenomena in optical physics. Here we show that unique optical properties of metamaterials (MMs) open unlimited prospects to “engineer” light itself. We propose and demonstrate for the first time a novel way of complex light manipulation in few-mode optical fibers using optical MMs. Most importantly, these studies highlight how unique properties of MMs, namely the ability to manipulate both electric and magnetic field components of electromagnetic (EM) waves, open new degrees of freedom in engineering complex polarization states of light at will, while preserving its orbital angular momentum (OAM) state. These results lay the first steps in manipulating complex light in optical fibers, likely providing new opportunities for high capacity communication systems, quantum information, and on-chip signal processing.

Many ways to increase optical communication capacity are already being used to achieve 100 Tb/s, including novel modulation formats, time and wavelength division multiplexing, and linear polarization states<sup>1–5</sup>. The only remaining unused dimension is the spatial degree of freedom. As a result, space division and/or mode division multiplexing emerge as the remaining breakthrough technologies<sup>6–9</sup>. The central idea of these approaches is transmitting data using multiple orthogonal propagation modes of a multi-core fiber or multimode fiber. To date, the first attempts to realizing these approaches were to design specialty fibers<sup>10–12</sup>. Despite all the impressive progress in this direction, the continuously growing demand for ultra-fast, compact, all-optical signal processing and further increase in network capacity necessitates the quest for fundamentally new ways of light manipulation using yet unexploited degrees of freedom.

Here we propose and demonstrate for the first time a novel way of light manipulation in existing commercially available optical fibers. The key idea of our approach is to combine the advantages of three very different but remarkably complimentary technologies: i) few-mode optical fibers as a transmission medium, ii) structured light, or light with nontrivial states of polarization and orbital angular momentum (OAM), and iii) optical MMs, offering unparalleled opportunities for light manipulation.

Why few-mode fibers? Until now, implementation of mode multiplexing in the existing long-haul optical fiber systems has been hindered by the fact that these systems are based on single-mode fibers at the commonly used near-infrared wavelengths. However, the same fibers support a few or multiple modes at visible wavelength.

Why use structured light? As mentioned above, the only remaining unused dimension that could further boost the capacity of future communication systems is the spatial degree of freedom. This includes cylindrical vector beams (CVB) with nontrivial polarization states, including radially and azimuthally polarized beams and light carrying the OAM. The inherent orthogonality of the modes with different OAM allows them to be multiplexed and demultiplexed efficiently. OAM multiplexing is also compatible with polarization- and wavelength-multiplexing. The first steps in this direction date back to early 2000s when it was shown that the entanglement of OAM states could be used for quantum<sup>13</sup> and classical communications<sup>14</sup>. One of the major challenges in exploiting OAM is that the complete set of fiber eigenmodes should be independently addressed at the transmitter and extracted at the receiver and most mode coupling effects inside the fiber should be solved. While several impressive initial results were reported on propagation of either CVBs or OAM modes in specially designed fibers, the question is whether unique properties of CVBs and OAM modes could be combined to ensure stable propagation of such beams in a conventional few mode fiber. Although we do not answer this question yet, as a first step we investigate how such modes can be coupled, manipulated and outcoupled using on-fiber MMs based components.

This brings us to the question that inspired this study: can we use the unparalleled opportunities offered by optical MMs to manipulate structured light in an all-fiber environment? Here, we show the first steps towards the



development of *MMs fabricated on the input and/or output ends of the fiber enabling efficient coupling and manipulation of structured light propagating in a few-mode fiber.*

Metamaterials have attracted a lot of attention recently because of the possibilities offered by their unusual properties such as negative index of refraction and magnetism at optical frequencies<sup>15–19</sup>. To date, the majority of studies have focused on plane wave or Gaussian beam propagation in MMs<sup>20</sup>. However, optical interactions of structured light, such as radially or azimuthally polarized vector beams, spiraling beams – optical vortices, and other beams carrying spin and orbital angular momenta, with optical MMs are largely unexplored. The vector nature of light-matter interactions is of significant interest from both fundamental and application viewpoints, including data storage, optical communications, materials sciences, and astronomy. On the other hand, vortices have been discovered in many different areas of physics, including such diverse fields as photonics, plasma physics, fluid dynamics, or atmospheric physics. In particular, optical applications of these fascinating states of light include optical tweezers used to manipulate small particles or biological cells<sup>21</sup>, nanofabrication, where the vortices helicity is transferred to metal producing chiral metal nanoneedles<sup>22,23</sup>, and finally, in astronomy for the observation of very dim objects near very bright objects, such as extrasolar planets near their host star<sup>24,25</sup>.

Recent developments in the field of MMs and transformation optics have enabled several paradigm shifts in modern photonics including magnetism at optical frequencies, backward waves, unprecedented control over light propagation through the "engineering" of space for light and more recently the light itself<sup>26–41</sup>.

In this study we demonstrate unique opportunities for vector vortex beam manipulation using fiber-integrated magnetic MMs. First of all, it should be noted that the magnetic susceptibility of most natural materials is very small compared to the dielectric susceptibility of these materials, thus limiting the interaction of atoms to the electric component of the electromagnetic (EM) wave, leaving the magnetic component largely unexploited. As a result, the magnetic permeability,  $\mu$ , is close to 1 for many naturally existing materials. Magnetism is particularly weak at optical frequencies because the

relaxation times of paramagnetic and ferromagnetic processes are significantly longer than the optical period, and thus the electron movement in atoms is the only mechanism for the magnetic response. As a result, the magnetic field component is usually not involved in light-matter interactions. Such extremely weak magnetism is mainly due to limitations of the material properties imposed by their constituent components – atoms and molecules. On the contrary, MMs are built of so-called "meta" atoms that are properly engineered resonant nanostructures that enable the realization of, in principle, any values of magnetic permeability.

## Results

Magnetic MMs were fabricated on the transverse cross section of a SM800 fiber that is a "few-mode fiber" at 633 nm and consisted of the periodic three-layered Ag-LiF-Ag nanostripes made using focused ion beam (see Supplementary information for details on deposition and patterning). The entire cross-section of the fiber was covered by the metal-dielectric-metal multilayer and the pattern was made such that it completely covered the fiber core (shown by black circle in Fig. 1a), ensuring that all light coupled to the core interacts with the MMs and no light is transmitted through the unpatterned area. Figure 1(b) shows a schematic of the cross-section of two nanostripes and two distinct orientations of linearly polarized light. The incoming wave is said to be TM polarized if the wave vector  $k$  is pointing down as shown on Fig. 1(b), the incident electric field  $E$  is parallel to the cross-section of the nanostripes, and the incident magnetic field  $H$  is perpendicular to the plane of the cross-section. In this case, the incident light at a particular wavelength excites a magnetic resonance, as was discussed in detail in our previous work<sup>42,43</sup>. The thickness, spacing and the average width of top and bottom nanostripe cross-sections (Fig. 1c) determine the wavelength at which magnetic resonance occurs<sup>42</sup>. The basic principle behind such a resonant property is as follows. If the electric field is parallel to the cross-section of the nanostripes ( $E$  along the  $x$ -axis in Fig. 1d) the magnetic field is oriented perpendicular to the plane of the nanostripes ( $H$  along the  $y$ -axis in Fig. 1d), and it would excite

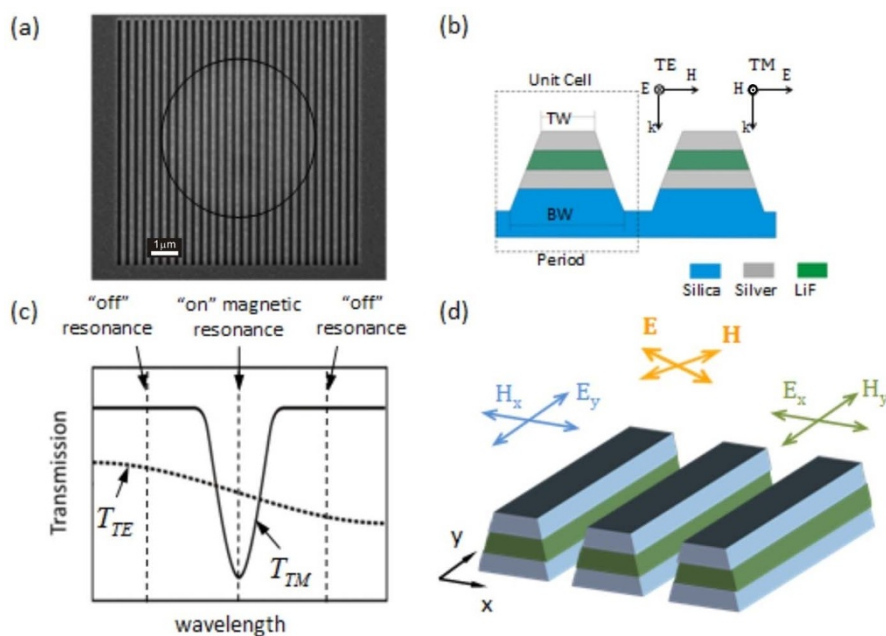


**Figure 1** | (a) The SEM image of magnetic metamaterial covering the core of the fiber (shown by a solid line); (b) Schematic cross-section of two metamagnetic nanostripes consisting of a Ag-LiF-Ag multilayer on silica fiber as a substrate, incoming light  $k$ ,  $E$ , and  $H$  fields orientation is also shown for the cases of TE and TM linearly polarized light; TW-top width, BW-bottom width; (c) Schematic of transmission spectra for TE and TM polarization; (d) Schematic of metamagnetic structure illuminated with light linearly polarized at an angle to the grating axes.



anti-parallel currents (antisymmetric plasmon polariton wave) in the pair of nanostrips. Near such resonance, the effective magnetic permeability of the structure changes sign and this resonant behavior corresponds to a minimum in the transmission spectrum as shown in Fig. 1(c). On the other hand, no resonant behavior is expected in the case of the so-called TE polarized wave, when the magnetic field of the incident wave is parallel to the cross-section of the nanostrips ( $H$  along the  $x$ -axis in Fig. 1d) and the electric field is parallel to the length of nanostrips ( $H$  along the  $y$ -axis in Fig. 1d). Therefore, no minima in transmission spectrum should be expected in this case and the structure behaves as a dilute metal showing higher transmission at shorter wavelengths (Fig. 1c). Essentially, apart from the novel engineered magnetic response such, an array of nanostrips operates as a wire grid polarizer that predominantly passes through the electric field component of light oscillating perpendicular to the wires (TM-polarized wave). However, the picture of light interaction with such nanostructures completely changes when the structure is designed to couple to the magnetic field component of incoming light. Until now, most of the studies of magnetic MMs focused on either pure TE or pure TM polarized plane wave transmission. Here, we show that remarkably new effects take place when such structures are exposed to vector vortex beams. Before discussing the experimental and modeling results, let's qualitatively predict the effect of the metamagnetic structure on light linearly polarized at an angle to the grating axes, as shown in Fig. 1(d):

- i. At wavelengths “off” magnetic resonance, the “linear polarizer”, predominantly affecting the electric field component aligned with the nanostrips  $E_y$  component (projection of E-field along  $y$ -axis), is expected to dominate;
- ii. At wavelengths close to the magnetic resonance, the electric field component aligned with the nanostrips  $E_y$  would still be affected by the same “linear polarizer” effect, but now, the presence of the magnetic resonance would result in an effective “magnetic polarizer” that would pass the  $H_x$  component (projection of H-field along  $x$ -axis) and reduce the magnetic field component parallel to the nanostrips  $H_y$  and corresponding  $E_x$  component. As a result both polarizers would affect light propagation.
- iii. Exactly at resonance, the “magnetic polarizer” effect is expected to be the strongest and it would predominantly pass the  $H_x$  component.

In order to validate these predictions, we designed and fabricated three groups of magnetic MM samples on fiber: Group 1,

“on-resonance samples”, was designed such that the magnetic resonance coincides with the wavelength of the HeNe laser source ( $\lambda = 633$  nm); Group 2, “off-resonance samples,” was designed such that the 633 nm corresponded to an off-resonance spectral range; and Group 3, “reference samples,” was fabricated such that those samples have the same pitch/period parameters as the on-resonance group, but consisted of only one metal layer with the same total metal thickness as other samples. Group 3 samples were used to confirm the origin of the magnetic resonance due to the three-layer MMs structure, i.e. in reference samples with no multilayer, no magnetic resonance was observed. The parameters and transmission spectra for Group 1 and 2 are shown in Supplementary Materials.

A radially polarized vortex beam was generated by transmitting a circularly polarized beam through a subwavelength metallic concentric ring pattern fabricated on the cross-section of a few-mode fiber, as shown in Fig. 2(a)–(c)<sup>44,45</sup>. The concentric ring pattern transmits the radial component of the beam and blocks the azimuthal component (Fig. 2d). Using Jones matrix formalism we find that if we consider initially Left Hand Circular polarized light being transmitted through such ring pattern, the transmitted beam would be a radially polarized vortex beam with OAM of 1:

$$\begin{aligned}
 E_{LHC} &= \frac{1}{\sqrt{2}} P(r) (\mathbf{e}_x \ \mathbf{e}_y) \begin{pmatrix} 1 \\ i \end{pmatrix} \\
 &= \frac{1}{\sqrt{2}} P(r) [\cos(\varphi) \mathbf{e}_r - \sin(\varphi) \mathbf{e}_\varphi \ \sin(\varphi) \mathbf{e}_r + \cos(\varphi) \mathbf{e}_\varphi] \begin{pmatrix} 1 \\ i \end{pmatrix} \quad (1) \\
 &= \frac{1}{\sqrt{2}} P(r) e^{i\varphi} (\mathbf{e}_r \ \mathbf{e}_\varphi) \begin{pmatrix} 1 \\ i \end{pmatrix}
 \end{aligned}$$

First, the MM fiber was removed in order to observe and characterize the vortex itself. Using a CCD camera we observed a donut-shaped beam (Fig. 2e) at the output of a setup schematically shown in Fig. 2(a). However, it should be mentioned that an observation of a donut-shaped intensity profile does not prove that the cylindrical beam carries any topological charge. The presence of a singularity can be observed by overlapping a vortex beam with a spherical wave, resulting in a spiral interference pattern shown in Fig. 2(f), or with a tilted plane wave, resulting in a fork-like interference pattern.

Next, we numerically and experimentally studied interactions of radially polarized optical vortices with magnetic MM structures. Figure 3(a) shows the schematic of the experimental setup. Calculated and measured intensity profiles and calculated instantaneous polarization vector distributions for the case of off-resonance

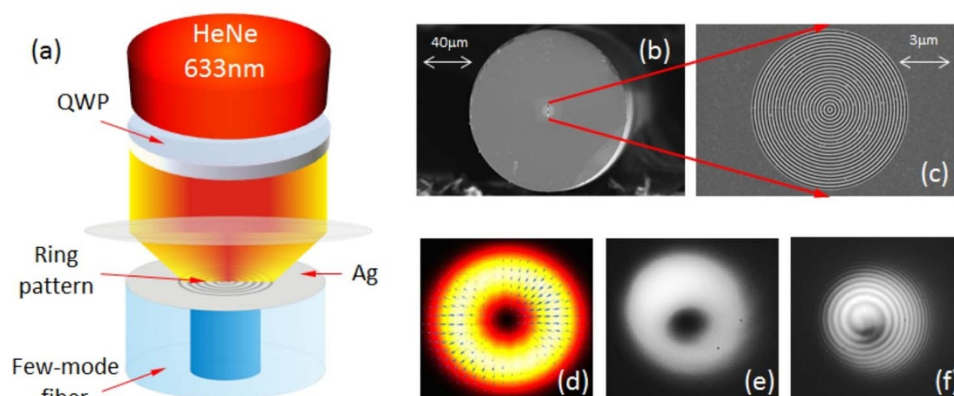


**Figure 2** | (a) The schematic of the setup for generation of a radially polarized vortex beam; (b)–(c) The SEM images of the concentric rings pattern on fiber covered with 200 nm thick Ag layer, such that the patterned area had a pitch/period ratio of 100 nm/200 nm; (d) Calculated intensity and polarization distribution of the resulting beam; (e) Measured intensity profile of the generated radially polarized vortex beam; (f) Measured interference pattern resulting from overlapping the generated vortex beam with a spherical reference beam.



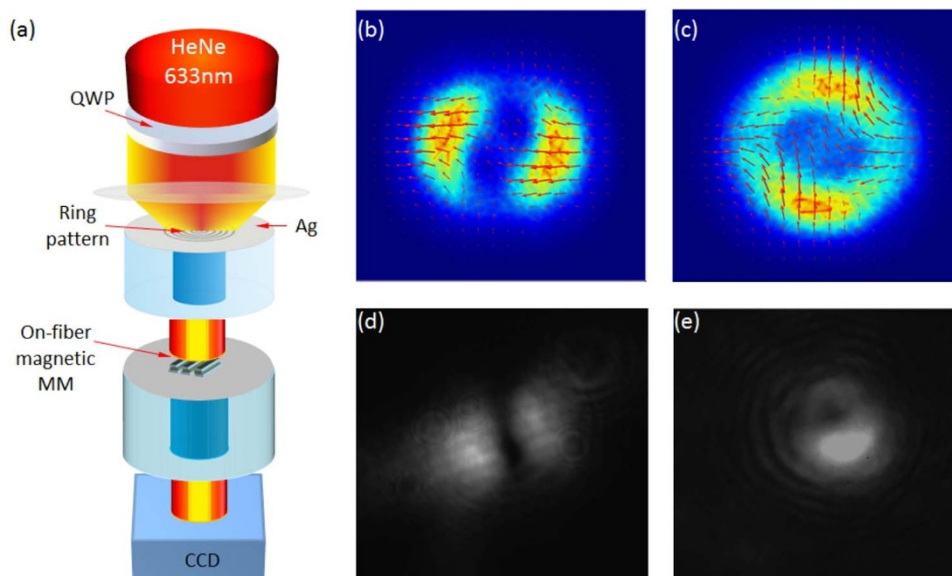


**Figure 3** | (a) The schematic of the experimental setup to study radially polarized vortex beam interaction with the magnetic MM; (b) and (c) Calculated intensity profiles at the output for the cases of off- and on-resonance propagation, respectively; (d) and (e) Measured intensity profiles at the output for the cases of off- and on-resonance propagation, respectively.

interaction are shown in Fig. 3(b) and (d), respectively, and for the case of on-resonant interaction in Fig. 3(c) and (e), respectively. Calculated polarization distributions support our earlier prediction that while in the off-resonance case, the magnetic MM acts similar to a wire polarizer that converts radially polarized beam into a nearly linearly polarized one (Fig. 3b), significantly more complex polarization states can be obtained in an on-resonance case due to coupling of both electric and magnetic field components of light to the structure. However, we note that experimentally recorded intensity profiles do not provide sufficient information about the physics of the light-matter interaction. Therefore, next we comprehensively studied polarization state and OAM characteristics of the output beam.

First we investigated the output polarization state and intensity profiles after the incident radially polarized vortex beam interacted with the off- and on- resonance magnetic MM. In order to analyze the state of polarization, we inserted a rotating analyzer just before the CCD (both in numerical simulations and in experiments). The results of these studies are shown in Fig. 4 and can be summarized as follows: i) in the off-resonance case, the MM structure acts mainly as a grating polarizer resulting into a 2-lobes pattern with a major dark-line remaining in the same direction independent of the position of the linear polarizer (analyzer); ii) in the on-resonance case, the pattern evolves from a 2-lobes pattern to a nearly donut shaped pattern with a major dark-line rotating with the analyzer.

## Discussion

Figure 4 shows the measured and calculated evolution of the beam profile and local instantaneous polarization direction obtained in numerical simulations as a function of the angle of rotation of the analyzer. In both the experiments and simulations it is assumed that  $\theta = 0^\circ$  corresponds to a vertically positioned high-transmission axis of the analyzer, which means that we expect to observe high transmission of the bright lobes in Fig. 4 for the on-resonance case, and low transmission of the bright lobes in the off-resonance case. From experiments we find that the direction of the dark-line for the off-resonance sample is nearly unchanged as a function of angle, while the direction of dark-line for on-resonance sample is rotating. In addition, we performed the same analysis using a reference sample that has the same pitch/period as the on-resonance sample but only one 90 nm Ag layer. We found

that the results of light interaction with the reference sample are identical to those in the case of the off-resonance sample. This proves our prediction that in an off-resonance the MM mainly acts as a wire polarizer and once again confirms that the magnetic resonance that originates from the metal-dielectric-metal structure is strongly wavelength dependent and dominates in the on-resonance radially polarized vortex-MM interaction. Note that while excellent agreement between experimental and modeling results is observed in the on-resonance case (intensity pattern rotation follows the analyzer rotation), in the off-resonance case good qualitative agreement is found for the range of angles from  $30^\circ$  to  $105^\circ$  in that the intensity pattern is not rotating, while at other angles some rotation direction of the intensity pattern is observed. The apparent mismatch between the experiments and simulations could be understood as follows. For an ideal wire polarizer and no magnetic resonance effect, we would expect to observe the dark-line in exactly the vertical direction, at all angles of rotation of the analyzer in both the experimental and numerical cases. However, there are several factors that could contribute to the deviation from vertical direction of the dark-line orientation. In the experiments, this deviation is likely to originate from an imperfect alignment of the sample. In simulations, the deviation could be explained as follows. While the “wire polarizer” effect dominates in the off-resonance case, the magnetic permittivity in the vicinity of the resonance does not reach 1 and, therefore, still enables some magnetic field coupling to the structure. Thus, the rotating pattern that we observe in numerical simulations is due to incomplete vanishing of the magnetic resonance effect. The intensity of the rotating part of the beam however, is much lower than that in the bright intensity lobes and thus was not easily observable in the images captured by the CCD camera in the experimental studies. Clear indication of the presence of those additional lobes in the experimental result can be seen at  $0^\circ$  and  $165^\circ$ . In the range of angles from  $30^\circ$  to  $105^\circ$  the effect of wire polarizer dominates but the effect of magnetic resonance still contributes to the overall intensity pattern resulting in some rotation of the dark-line. However, the most important conclusion following from these studies is that in the off-resonance case the direction of the dark-line does not follow the rotation of the analyzer, while the absolute value of the fixed angle may deviate from zero degrees with respect to the vertical direction.

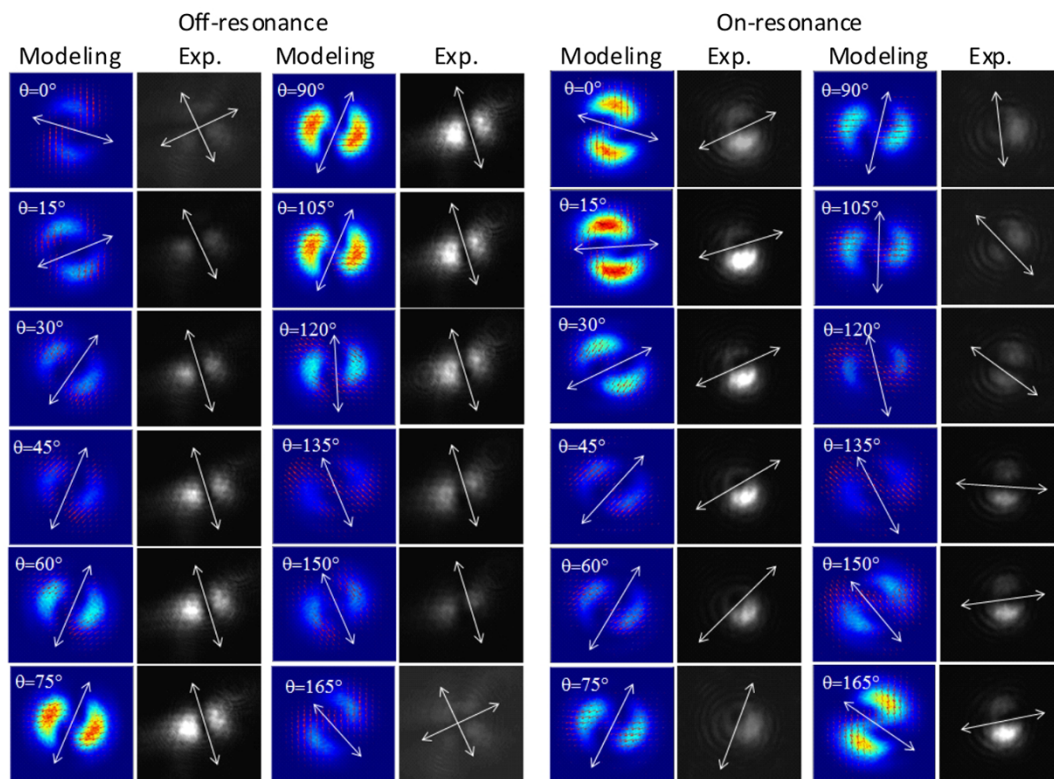


**Figure 4** | Calculated (Modeling) and measured (Exp.) evolution of intensity profiles and instantaneous local polarization direction (numerical simulations) of an initially radially polarized vortex beam after its interaction with the magnetic metamaterial off- (left) and on- (right) magnetic resonance with a polarization analyzer inserted between the fiber with MM and a CCD camera.

Finally, comparing the interference patterns of the original radially polarized vortex with a spherical reference beam, and those transmitted through the on-resonance and off-resonance magnetic MMs, we conclude that neither on-resonance, nor off-resonance interactions of the radially polarized vortex beam with magnetic MMs changes the OAM state of the incident beam (spiral interference patterns are shown in supplementary materials). Indeed, it was previously shown that although spin-to-orbit conversion can be achieved using subwavelength structures including subwavelength gratings, such conversion relies on space-variant phase modification induced by transversely inhomogeneous gratings or on discontinuities in the spatial profile of the subwavelength structures<sup>46–48</sup>. The subwavelength structure of the magnetic MMs considered here is space-invariant and contains no discontinuities. Therefore, the OAM of the incoming beam is preserved, while its complex polarization state can be manipulated independently by tuning the spectral characteristics of the structure around magnetic resonance.

In summary, we designed and demonstrated an all-fiber based complex light-MM system and performed a detailed study of the interactions of a radially polarized vortex beam with magnetic MMs. Our studies indicate that propagation of a radially polarized vortex beam in magnetic MMs results in changes of the polarization state of the beam on- and off- magnetic resonance that can be designed and controlled with very high precision, while orbital angular momentum remains intact. Most importantly, these studies highlight how unique properties of MMs, namely the ability to manipulate both electric and magnetic field components of EM waves open new degrees of freedom in engineering complex polarization states of light at will, while preserving the OAM state. These results represent the first steps in manipulating complex light in optical fibers, likely providing new opportunities for multidimensional communication, quantum information, optical trapping and on-chip signal processing.

## Methods

**Deposition.** Both the concentric rings structures and magnetic MMs structures were fabricated on the transverse cross section of a SM800 fiber. 10 cm long pieces of fiber were cleaved using a high precision fiber cleaver (CT-32) with a typical cleave angle of  $\pm 0.5^\circ$ . Well cleaved fibers were cleaned under a standard acetone-methanol-deionized water ultrasonic cleaning procedure. The 200 nm Ag or metal-dielectric-metal layers were deposited in a customized Angstrom evaporation system. In order to improve the adhesion of the Ag layers, a two nanometer thick Titanium (Ti) layer was deposited on the fiber cross-section surface by electron beam evaporation. Standard electron beam evaporation was used to deposit the 30 nm Ag layers. 30 nm LiF was deposited by thermal evaporation.

**Patterning.** Optical fibers with the metal or metal-dielectric-metal coating were mounted on the  $45^\circ$  side of a standard  $45^\circ$  stub by using carbon tape. Alignment markers, which were not necessary for concentric rings fiber, were put on the jacket of each MMs fiber to indicate the nanostrips' direction for future experiments. These markers made it easier to determine the TE and TM polarization mode of MMs for the propagating light. The patterns were made by focus ion beam (FIB) in a Zeiss AURIGA CrossBeam Workstation (FIB-SEM). A pattern area of  $8 \mu\text{m} \times 8 \mu\text{m}$  (radius  $4 \mu\text{m}$  for concentric ring pattern) ensured that the entire core area of the fiber was covered. The parameters of the resulting patterns were then measured using scanning electron microscopy (SEM) before the sample was removed from the AURIGA.

1. Agrawal, G. P. *Fiber-Optic Communication Systems*, 3rd ed. (Wiley-Interscience, Hoboken, New Jersey 2010).
2. Gnauck, A. H., Tkach, R. W., Chraplyvy, A. R. & Li, T. High-capacity optical transmission systems. *J. Lightwave Technol.* **26**, 1032–1045 (2008).
3. Essiambre, R. J. & Tkach, R. W. Capacity trends and limits of optical communication networks. *Proc. IEEE* **100**, 1035–1055 (2012).
4. Gnauck, A. H. *et al.* Spectrally efficient long-haul WDM transmission using 224-Gb/s polarization-multiplexed 16-QAM. *J. Lightwave Technol.* **29**, 373–377 (2011).
5. Zhou, X. *et al.* 64-Tb/s, 8 b/s/Hz, PDM-36QAM transmission over 320 km using both pre- and post-transmission digital signal processing. *J. Lightwave Technol.* **29**, 571–577 (2011).
6. Richardson, D. J., Fini, J. M. & Nelson, L. E. Space-division multiplexing in optical fibres. *Nature Photonics* **7**, 354–362 (2013).
7. Fini, J. M. *et al.* High-Capacity Space-Division-Multiplexed DWDM Transmissions Using Multicore Fiber. *J. Lightwave Technol.* **30**, 486–492 (2012).



8. Liu, X. *et al.* 1.12-Tb/s 32-QAM-OFDM superchannel with 8.6-b/s/Hz intrachannel spectral efficiency and space-division multiplexed transmission with 60-b/s/Hz aggregate spectral efficiency. *Opt. Express* **19**, B958–B964 (2011).
9. Ryf, R. *et al.* Mode-division multiplexing over 96 km of few-mode fiber using coherent  $6 \times 6$  MIMO processing. *J. Lightwave Technol.* **30**, 521–531 (2012).
10. Bozinovic, N. *et al.* Terabit-Scale Orbital Angular Momentum Mode Division Multiplexing in Fibers. *Science* **340**, 1545–1548 (2013).
11. Bozinovic, N., Golowich, S., Kristensen, P. & Ramachandran, S. Control of orbital angular momentum of light, with optical fibers. *Opt. Lett.* **37**, 2451–2453 (2012).
12. Gregg, P. *et al.* Stable Transmission of 12 OAM States in Air-Core Fiber, in CLEO: 2013, OSA Technical Digest (online) (Optical Society of America, 2013), paper CTu2K.2.
13. Mair, A., Vaziri, A., Weihs, G. & Zeilinger, A. Entanglement of the orbital angular momentum states of photons. *Nature* **412**, 313–316 (2001).
14. Gibson, G. *et al.* Free-space information transfer using light beams carrying orbital angular momentum. *Opt. Express* **12**, 5448–5456 (2004).
15. Pendry, J. B. & Smith, D. R. Metamaterials and Negative Refractive Index. *Science* **305**, 788–792 (2004).
16. Shalaev, V. M. Optical negative-index metamaterials. *Nature Photonics* **1**, 41–48 (2007).
17. Shalaev, V. M. Transforming light. *Science* **322**, 384–386 (2008).
18. Litchinitser, N. M., Gabitov, I. R., Maimistov, A. I. & Shalaev, V. M. Negative Refractive Index Metamaterials in Optics. *Progress in Optics* **51**, 1–68 (2008).
19. Soukoulis, C. M. & Wegener, M. Past achievements and future challenges in the development of three-dimensional photonic metamaterials. *Nature Photonics* **5**, 523–530 (2011).
20. Alali, F. & Litchinitser, N. M. Gaussian Beams in Near-Zero Transition Metamaterials. *Opt. Commun.* **291**, 179–183 (2013).
21. Padgett, M. & Bowman, R. Tweezers with a twist. *Nature Photonics* **5**, 343–348 (2011).
22. Toyoda, K. *et al.* Transfer of Light Helicity to Nanostructures. *Phys. Rev. Lett.* **110**, 143603 (2013).
23. Toyoda, K., Miyamoto, K., Aoki, N., Morita, R. & Omatsu, T. Using Optical Vortex to Control the Chirality of Twisted Metal Nanostructures. *Nano Lett.* **12**, 3645–3649 (2012).
24. Foo, G., Palacios, D. M. & Swartzlander, G. A. Jr. Optical vortex coronagraph. *Opt. Lett.* **30**, 3308–3310 (2005).
25. Swartzlander, G. A. Jr. Astronomical demonstration of an optical vortex coronagraph. *Opt. Express* **16**, 10200–10207 (2008).
26. Pendry, J. B., Schurig, D. & Smith, D. R. Controlling electromagnetic fields. *Science* **312**, 1780–1782 (2006).
27. Leonhardt, U. Optical Conformal Mapping. *Science* **312**, 1777–1780 (2006).
28. Schurig, D. *et al.* Metamaterial electromagnetic cloak at microwave frequencies. *Science* **314**, 977–980 (2006).
29. Cai, W., Chettiar, U. K., Kildishev, A. V. & Shalaev, V. M. Optical cloaking with metamaterials. *Nature Photonics* **1**, 224 (2007).
30. Litchinitser, N. M., Maimistov, A. I., Gabitov, I. R., Sagdeev, R. Z. & Shalaev, V. M. Metamaterials: electromagnetic enhancement at zero-index transition. *Opt. Lett.* **33**, 2350–2353 (2008).
31. Rahm, M. *et al.* Design of electromagnetic cloaks and concentrators using form-invariant coordinate transformations of Maxwell's equations. *Photonics and Nanostructures - Fundamentals and Applications* **6**, 87 (2008).
32. Kildishev, A. V. & Shalaev, V. M. Engineering space for light via transformation optics. *Opt. Lett.* **33**, 43–45 (2008).
33. Smolyaninov, I. I., Smolyaninova, V. N., Kildishev, A. V. & Shalaev, V. M. Anisotropic Metamaterials Emulated by Tapered Waveguides: Application to Optical Cloaking. *Phys. Rev. Lett.* **102**, 213901 (2009).
34. Litchinitser, N. M. Structured Light meets Structured Matter. *Science* **337**, 1054–1055 (2012).
35. Zhao, Z., Wang, J., Li, S. & Willner, A. E. Metamaterials-based broadband generation of orbital angular momentum carrying vector beams. *Opt. Lett.* **38**, 932–934 (2013).
36. Yu, N. *et al.* Light propagation with phase discontinuities: Generalized laws of reflection and refraction. *Science* **334**, 333–337 (2011).
37. Kildishev, A. V., Boltasseva, A. & Shalaev, V. M. Planar Photonics with Metasurfaces. *Science* **339**, 1232009 (2013).
38. Ni, X., Emani, N. K., Kildishev, A. V., Boltasseva, A. & Shalaev, V. M. Broadband Light Bending with Plasmonic Nanoantennas. *Science* **335**, 427 (2012).
39. Shitrit, N. *et al.* Spin-Optical Metamaterial Route to Spin-Controlled Photonics. *Science* **340**, 724–726 (2013).
40. Yin, X., Ye, Z., Rho, J., Wang, Y. & Zhang, X. Photonic Spin Hall Effect at Metasurfaces. *Science* **339**, 1405–1407 (2013).
41. Sun, J., Zeng, J. & Litchinitser, N. M. Twisting light with hyperbolic metamaterials. *Opt. Express* **21**, 14975–14981 (2013).
42. Cai, W. *et al.* Metamagnetics with rainbow colors. *Opt. Express* **15**, 3333–3341 (2007).
43. Wang, X. *et al.* Optical fiber metamagnetics. *Opt. Express* **19**, 19813–19821 (2011).
44. Zhan, Q. Cylindrical vector beams: from mathematical concepts to applications. *Adv. Opt. Photon.* **1**, 1–57 (2009).
45. Chen, W., Han, W., Abeyinghe, D. C., Nelson, R. L. & Zhan, Q. Generating cylindrical vector beams with subwavelength concentric metallic gratings fabricated on optical fibers. *J. Opt.* **13**, 015003 (2011).
46. Bomzon, Z., Biener, G., Kleiner, V. & Hasman, E. Radially and azimuthally polarized beams generated by space-variant dielectric subwavelength gratings. *Opt. Lett.* **27**, 285–287 (2002).
47. Bomzon, Z., Biener, G., Kleiner, V. & Hasman, E. Space-variant Pancharatnam-Berry phase optical elements with computer-generated subwavelength gratings. *Opt. Lett.* **27**, 1141–1143 (2002).
48. Nye, J. F. Polarization effects in the diffraction of electromagnetic waves: the role of disclinations. *Proc. R. Soc. London Ser. A* **387**, 105–132 (1983).

## Acknowledgements

The authors acknowledge useful discussions with Grover Swartzlander. This work was supported by US ARO under award # W911NF-11-1-0333.

## Author contributions

All authors contributed equally to the study, discussed the results and commented on the manuscript at all stages. N.L. and J.Z. formulated the idea of manipulation of light spin and orbital angular momentum using on-fiber MM structures and designed the experiments, J.Z. performed all experimental characterization of structured light-MM interactions, J.Z., J.S. and N.L. analyzed the data and developed theoretic models; X.W. and A.C. developed the fabrication process and prepared all metamaterial samples; J.S. and A.P. developed numerical modeling tools used to design MMs and analyze the experimental data; J.Z. and N.L. wrote the paper in discussion with all authors; A.C. evaluated the data and N.L. supervised the work.

## Additional information

Supplementary information accompanies this paper at <http://www.nature.com/scientificreports>

**Competing financial interests:** The authors declare no competing financial interests.

**How to cite this article:** Zeng, J. *et al.* Manipulating Complex Light with Metamaterials. *Sci. Rep.* **3**, 2826; DOI:10.1038/srep02826 (2013).



This work is licensed under a Creative Commons Attribution-NonCommercial-NoDerivs 3.0 Unported license. To view a copy of this license, visit <http://creativecommons.org/licenses/by-nc-nd/3.0>